Muonium

With the production and decay of muonium, one can measure hyperfine structure intervals, study weak interactions and observe a rich hydrogen-like chemistry.

by Vernon W. Hughes

MUONIUM IS THE atom consisting of a positive muon and an electron. In this article I review the work that has been done on muonium and has been reported in the literature. The work started about 10 years ago when parity nonconservation was discovered.

Reasons for interest

Muonium is of great interest in several subfields of physics. First, it is the simplest system involving the muon and the electron and hence is the best one for studying with precision the interaction of these two elementary particles. The muon is a particularly mysterious particle because it appears to behave in all respects like a heavy electron, and hence there appears to be no interaction which could account for the large ratio of the muon mass to the electron mass. Thus the muon occupies an anomalous role in the spectrum of the elementary particles. We have been able to study the electromagnetic interaction of the electron and the muon through a precise measurement of the hyperfine structure interval in the ground state of muonium.

Second, muonium is a light isotope of hydrogen in which the positive muon replaces the proton. Hence, muonium has a rich chemistry and its interactions with other atoms and molecules have been studied. Third, muonium provides a useful system for studying certain aspects of the weak interaction of the muon and electron, in particular a possible weak interaction coupling muonium to antimuonium, which is the atom consisting of a negative muon and a positron.

Table 1 lists the properties of the muon. The excellent agreement between the experimental and theoretical values of the anomalous magnetic moment factor provides the most critical proof that the muon is a heavy Dirac particle with the usual coupling to the electromagnetic field.

How we study it

The tool for studying muonium is provided by parity nonconservation in the weak interactions involved in the production and decay of the muon (see figure 1). The positive pi meson decays into a positive muon and a muon-type neutrino. In the rest frame of the pion the muon spin (indicated by the double line arrow), is in the direction opposite to its linear memen-tum, indicated by the single line arrow. This correlation of spin direction and velocity direction is a consequence of parity nonconservation and provides us with polarized muons. The positive muon decays into a positron and two neutrinos with a continuous positron

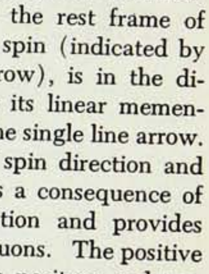

The author is professor in the physics department at Yale University. He has been consultant to Los Alamos Scientific Laboratory, Oak Ridge National Laboratory and the Institute for Space Studies of NASA. His major interests are in elementary-particle and atomic physics. This article was prepared from a lecture given at the Belfer Graduate School of Science, Yeshiva University.

energy spectrum extending up to 52 MeV. The angular distribution of the positrons with respect to the muon spin direction $I_{e^+}(\theta)$ is asymmetric because of parity nonconservation.

$$I_{e^+}(\theta) \propto 1 + A \cos \theta$$

θ is the angle between muon spin and direction of positron emission and A is approximately $+1/3$. So positrons are emitted preferentially along the muon spin direction. This characteristic of muon decay provides the means for detecting the muon spin direction.

Formation

The gross energy levels of muonium as given by the Schrödinger equation are the same as those of hydrogen except for a slightly different reduced-mass factor in the Rydberg constant.

Table 1. Properties of Positive Muon

Mass:	$m_\mu = (206.767 \pm 0.003)\ m_e$
Charge:	$+e$
Spin:	$I = 1/2$
Magnetic moment:	$\mu_\mu/\mu_p = 3.18338 \pm 0.0004$
Gyromagnetic ratio:	$g_\mu = 2(1.001162 \pm 0.000005)$
Lifetime (mean):	$\tau_\mu = (2.2000 \pm 0.0015)\ \mu$ sec

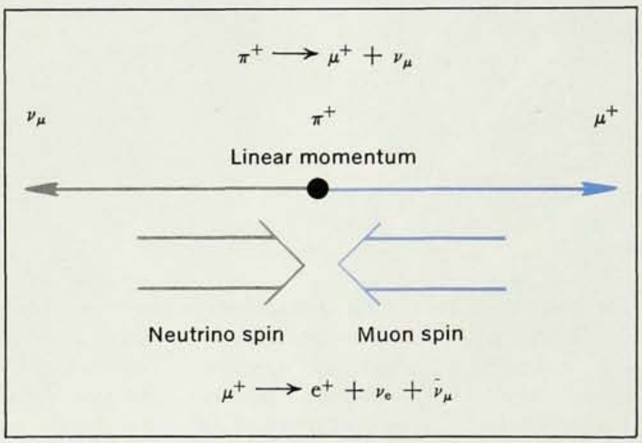

WEAK INTERACTIONS involved in the production and decay of the muon, demonstrating parity nonconservation. —FIG. 1

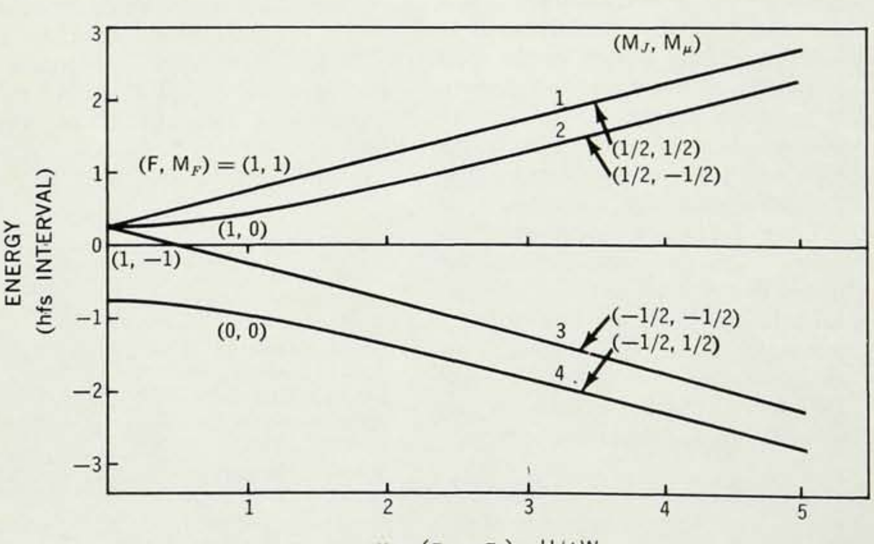

ENERGY-LEVEL DIAGRAM for hfs levels in ground state of muonium. At zero field, energy separation is the hfs interval–4463 MHz. —FIG. 2

Figure 2 shows the energy level diagram for the hyperfine structure levels in the ground $1\ {}^2S_{1/2}$ state of muonium. Energy in units of the hfs interval is plotted as a function of a dimensionless constant x, which is proportional to magnetic field. At zero magnetic field there are two levels—the upper triplet state with total-angular-momentum-quantum number $F = 1$ and the lower singlet state with $F = 0$. The energy separation is the hfs interval, which is due to the magnetic interaction between the spin magnetic moments of the electron and the muon. In an external magnetic field H the triplet state splits into its three magnetic substates designated by the magnetic quantum number M_F with the values $+1$, 0, and -1. At strong magnetic fields, when magnetic interactions of electron and muon magnetic moments with the external field is large compared to the hfs interval $(x \gg 1)$, the energy levels are as shown, and the good quantum numbers are M_J, the magnetic quantum number for the electron spin, and M_μ, the magnetic quantum number for muon spin. The states are numbered from 1 through 4 for convenience.

When positive muons are stopped in a gas, muonium is forced directly in its ground state by the capture of an electron by a positive muon. Argon has been used in most of our experiments

$$\mu^+ + Ar \rightarrow \mu^+e^- + Ar^+$$

This capture reaction has a maximum cross section for a muon kinetic energy of about 200 eV. Because the muons are polarized and the charge capture reaction is primarily due to the Coulomb interaction which does not alter the muon spin direction, polarized muonium is formed. If we have a strong magnetic field opposite to the direction of the muon beam and hence in the direction of the muon spins $M_\mu = +1/2$. Then only the two states $(M_J, M_\mu) = (+1/2, +1/2)$ and $(-1/2, +1/2)$ are formed. Half of the muonium atoms formed will be in each of these states. In a weak magnetic field polarized muonium is also formed. However, in weak magnetic fields M_μ is not a good quantum number, and the hfs interaction will partially depolarize the muons. So the distribution in the low field of states designated

(F, M_F) will be $(1, 1) = 1/2$, $(1, 0) = 1/4$, $(1, -1) = 0$, and $(0, 0) = 1/4$.

Discovery

The original search for muonium involved the attempt to observe its characteristic Larmor precession frequency in a weak external magnetic field. The Larmor precession frequency f_L of a magnetic moment μ associated with an angular momentum $F\hbar$ in an external magnetic field H perpendicular to μ is given by

$$f_L = \mu H / Fh$$

In a weak field the only muonium state formed that has a magnetic moment is the triplet state $(F, M_F) = (+1, +1)$. Since the magnetic moment is approximately the electron spin magnetic moment and $F = 1$, we then have

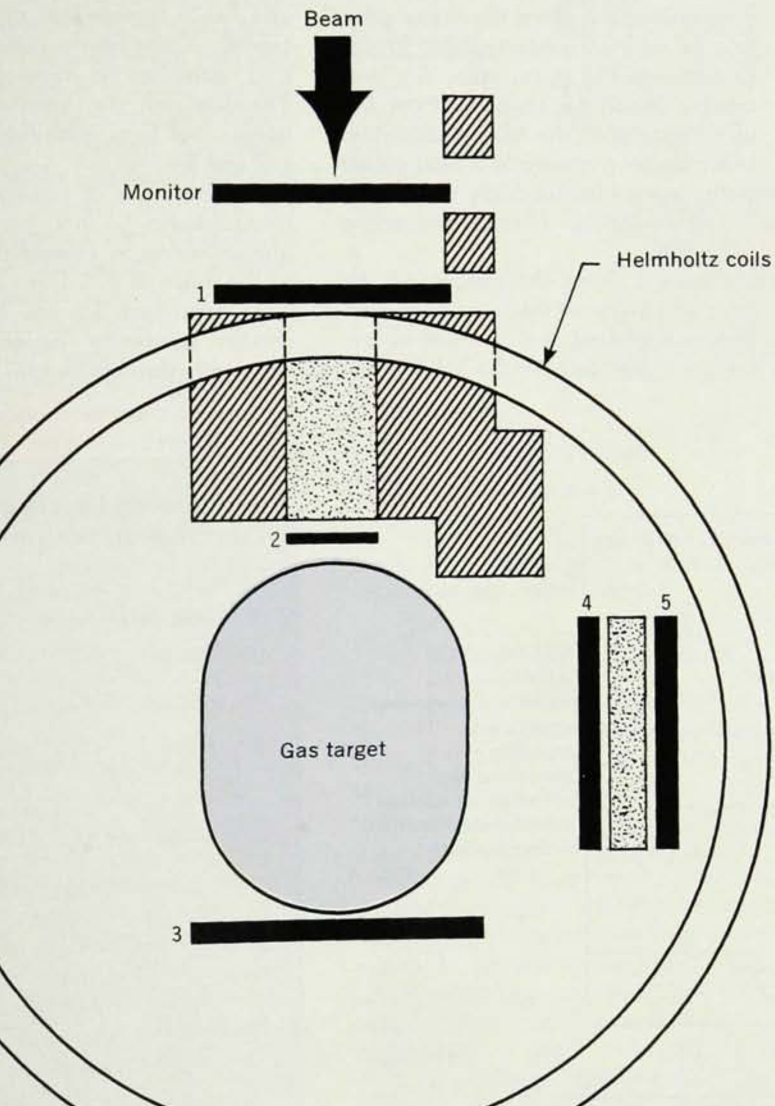

MUONIUM FORMATION. Experimental arrangement: **Helmholtz coils provide a field of 4 gauss perpendicular to the plane of the diagram.—FIG. 3**

Theoretical Formula for Hyperfine Structure Interval for Muonium

$$\Delta\nu = \left(\frac{16}{3}\alpha^2 c R_\infty \frac{\mu_\mu}{\mu_{e0}}\right) \times \left(1 + \frac{m_e}{m_\mu}\right)^{-3} \times \left(1 + \frac{3}{2}\alpha^2 + a_e + \epsilon_1 + \epsilon_2 + \epsilon_3 - \delta_\mu\right)$$

$$\mu_\mu = \mu_{\mu 0}(1 + a_\mu)$$

$$a_e = \frac{\alpha}{2\pi} - 0.328\frac{\alpha^2}{\pi^2}$$

$$a_\mu = \frac{\alpha}{2\pi} + 0.75\frac{\alpha^2}{\pi^2}$$

$$\epsilon_1 = \alpha^2 (\log 2 - 5/2)$$

$$\epsilon_2 = \frac{8\alpha^3}{3\pi}\log\alpha\,(\log\alpha - \log 4 + 281/480)$$

$$\epsilon_3 = \frac{\alpha^3}{\pi}(18.4 \pm 5)$$

$$\delta_\mu = \frac{3\alpha}{\pi}\,\frac{m_e m_\mu}{m_\mu^2 - m_e^2}\log\frac{m_\mu}{m_e}$$

$$\alpha^{-1} = 137.0388\ (\pm 9\text{ ppm})$$

$$\mu_e/\mu_p = 658.2106\ (\pm 1\text{ ppm})$$

$$\mu_\mu/\mu_p = 3.18338\ (\pm 13\text{ ppm})$$

$$R_\infty = 109737.31\text{ cm}^{-1}\ (\pm 0.1\text{ ppm})$$

$$c = 2.997925 \times 10^{10}\text{ cm/sec}\ (\pm 0.3\text{ ppm})$$

$$m_\mu/m_e = 206.761\ (\pm 25\text{ ppm})$$

$$\Delta\nu = 2.632942 \times 10^7\,\alpha^2 \times (\mu_\mu/\mu_p)\text{ MHz}\ (\pm 2\text{ ppm})$$

$$= 4\,463.16 \pm 0.10\text{ MHz}\ (\pm 22\text{ ppm})$$

The leading bracketed factor is the Fermi formula in which c = velocity of light, R_∞ = Rydberg constant, and μ_μ/μ_{e0} = ratio of muon magnetic moment to the electron Bohr magneton. The second factor is a reduced mass correction. The terms in the third bracket are relativistic, virtual radiative corrections, and relativistic recoil corrections (the latter based on the Bethe-Salpeter equation).

$$f_L = \mu_{e0}H/h = 1.40\ H\ \text{(MHz)}$$

Figure 3 shows the schematic diagram of the experiment. All our experiments have been done at the Columbia University Nevis synchrocyclotron. The 380 MeV proton beam strikes an internal target forming positive pi mesons which decay to positive muons, and an external meson beam is formed with a momentum of about 140 MeV/c. The meson beam has positive pions and positive muons. The pions are stopped in an absorber and muons with energies up to several MeV enter an argon gas target with a pressure of about 50 atmospheres. The muon loses energy by ionization and excitation of argon atoms and forms muonium stably with kinetic energies in the keV range. The muonium atom is then rapidly thermalized. The slowing down occurs in less than 10^{-9} sec. We had to purify the argon by recirculating it over titanium heated to about 700°C. The numbered black lines indicate scintillation counters, and the stopping of a muon in the gas target is indicated by a coincident 1, 2 but anticoincident 3 count. The Helmholtz coils which are indicated provide a magnetic field of about 4 gauss perpendicular to the plane of the diagram. The decay positrons are observed by the 4,5 counter telescope as coincident 4,5 counts and we measure the time delay of the positron count with respect to the time of the arrival of the muon. If polarized muonium is formed, the triplet $M_F = +1$ state should precess in the external magnetic field. Since the decay positron is emitted preferentially in the direction of the muon spin, this precession should be observed from the measurement of the time distribution of the decay positrons as a modulation of the muon lifetime decay curve with the characteristic Larmor precession frequency.

Figure 4 shows the analysis of the data; amplitude of the frequency component is plotted as a function of frequency. For case II the solid curve is the result of a least-squares Fourier analysis of the experimental data and the typical error bar corresponds to one standard deviation. The dashed curve is a theoretical line shape centered at the muonium precession frequency corresponding to the measured value of the magnetic field. With a field of 4.5 gauss a resonance is clearly seen at the predicted frequency. Similarly the resonance is seen for case III, with a different field of 3.9 gauss. As expected, no resonance is seen in case I when pions are stopped in the target and hence unpolarized muons are obtained. These results prove that polarized muonium is formed in argon. The data indicate that the fraction of muons that form muonium is between 1/2 and 1.

The existence of muonium with its characteristic Larmor precession frequency serves as a proof that the spin of the muon is $\hbar/2$ since the approximate expression for the Larmor precession frequency depends on the muon only through its spin value.

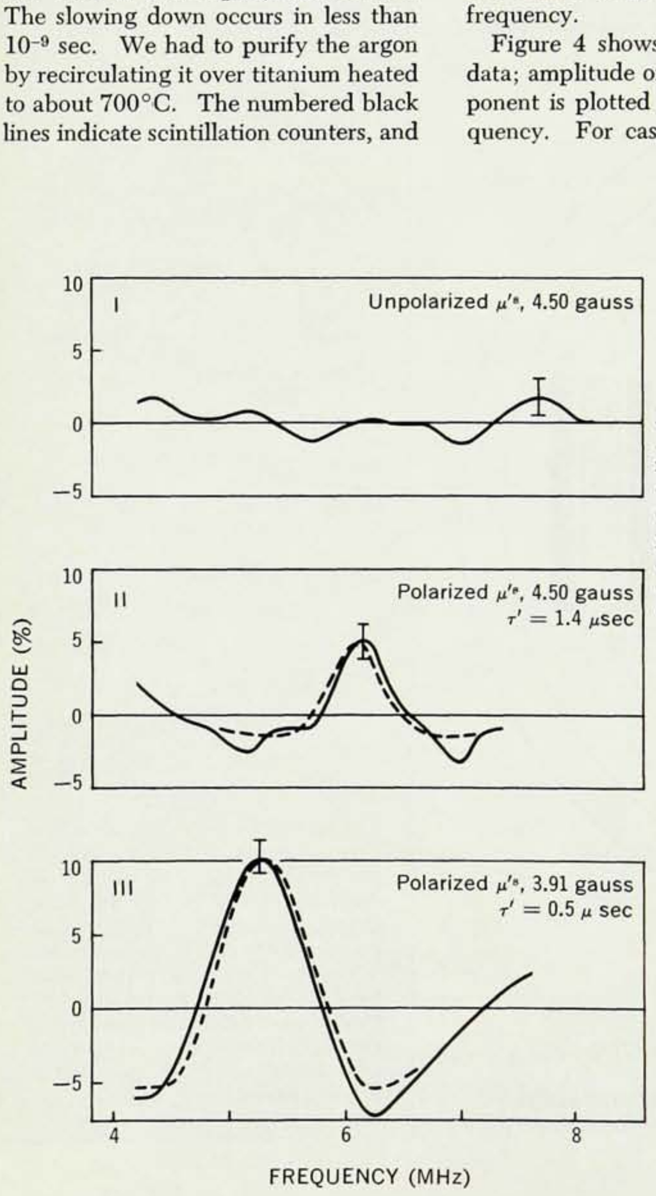

FREQUENCY ANALYSIS for muonium precession experiment. The quantity τ' is a parameter that accounts for various experimental sources of line breadth.
—FIG. 4

Energy Levels and Transition Frequencies

$$\mathcal{H} = a\mathbf{I}_\mu\cdot\mathbf{J} + \mu_{e0}g_J\mathbf{J}\cdot\mathbf{H} + \mu_{e0}g_\mu\mathbf{I}_\mu\cdot\mathbf{H}$$

the unit for g_μ is the same as for g_J

$$W_F = 1/2 \pm 1/2, M_F = -\frac{\Delta W}{4} \mp \mu_{e0}g_\mu H M_F \pm \frac{\Delta W}{2} \times (1 + 2M_F x + x^2)^{1/2}$$

$$x = \frac{(g_J - g_\mu)\mu_{e0}H}{\Delta W}$$

$$\nu\left[(M_J,M_\mu) = \left(\frac{1}{2},\frac{1}{2}\right) \rightarrow \left(\frac{1}{2},-\frac{1}{2}\right)\right]_{\text{strong field}} \approx \frac{a}{2} + \frac{\mu_{e0}g_\mu H}{h}$$

$$\nu\left[(F,M_F) = (1,1) \rightarrow (0,0)\right]_{\text{weak field}} \approx a + \frac{\mu_{e0}g_J H}{h}$$

Hfs interval: theory

In view of the results on muonium formation, we were encouraged to plan a precision magnetic resonance experiment to measure the hfs interval $\Delta\nu$. The box on page 31 gives the theoretical expression for $\Delta\nu$ under the assumption that the muon is a heavy electron. The expression is a perturbation theory series expansion in powers of the fine structure constant α and the ratio of the electron and muon masses. Values of the fundamental constants are shown, and the theoretical value is $\Delta\nu = 4463.16 \pm 0.10$ MHz. The error arises primarily from uncertainty in α which is taken from the old D fine structure measurement of Edwin Dayhoff, Sol Triebwasser and Willis E. Lamb, Jr, quoted with a limit of error of 9 parts per million. Important also is the uncertainty in the muon magnetic moment, which is obtained from a comparison of the muon and proton resonance frequencies in water.

The principle of the experiment is simple. Suppose we have a strong external static magnetic field H, along the spin direction of the incident muons; then muonium will be formed only in states 1 and 4 that have $M_\mu = +1/2$. If nothing is done to perturb this distribution of muonium states, the decay positrons will be emitted preferentially in the direction of H. However, suppose a microwave magnetic field is introduced with the proper Bohr frequency so it can induce a resonance transition of muonium from one hfs state to another, for example, from state 1 to state 2. In state 2 the muon spin points in the opposite direction, having $M_\mu = -1/2$, and the decay positrons from the state are emitted preferentially in the direction opposite to the direction of the static field. Hence an induced transition can be detected through the change in angular distribution of the decay positrons.

Transitions have been studied both at strong and weak magnetic fields. The box on page 32 gives the energy levels and transition frequencies. The Hamiltonian includes the hfs interaction, the interaction of the electron spin magnetic moment with the external magnetic field H, and the interaction of the muon spin magnetic moment with H. The energy levels are given by the Breit-Rabi formula whose solution is shown in figure 2. We take the viewpoint that the electron magnetic moment (or gyromagnetic ratio g_J) and the muon magnetic moment (or g_μ) are determined in other experiments so that the measurement of a single resonance transition determines the hfs interaction constant α, which is the only unknown. The transition observed at strong field is between states 1 and 2 with $(M_J, M_\mu) = (1/2, 1/2)$ and $(1/2, -1/2)$. The approximate frequency for this transition is the hfs interval divided by 2 plus the frequency associated with muon spin flip. At weak field we have observed the transition $(F, M_F) = (1, 1) \leftrightarrow (0, 0)$. The resonance frequency is approximately α plus a term associated with the electron spin flip.

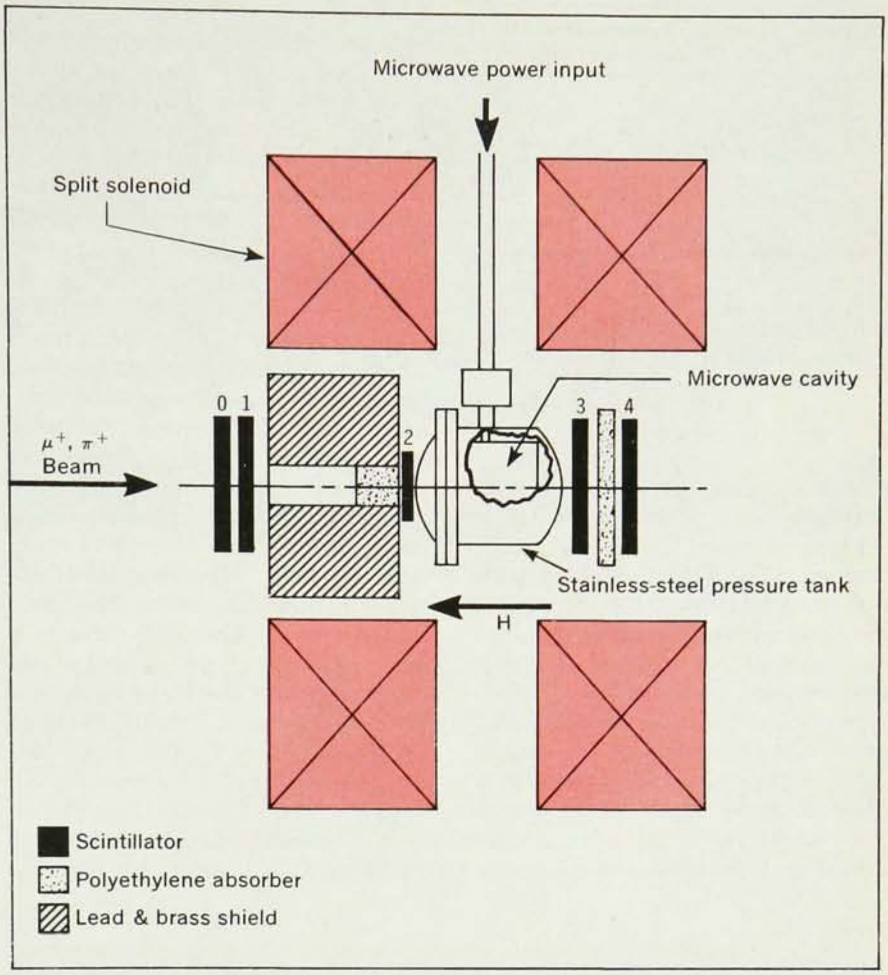

HIGH-FIELD ARRANGEMENT for hfs interval measurement involving an induced microwave transition. —FIG. 5

The box on page 35 gives the theoretical expression for the resonance line shape. A two-level problem can be considered with the energy separation being $\hbar\omega_0$. The equations for the state amplitudes a_p and a_q are given by the time dependent Schrödinger equation.

Hfs interval: experiment

Figure 5 shows the experimental setup. The muons are stopped in the high pressure argon target and indicated by coincident 1,2 but anticoincident 3 counts. A split solenoid provides a strong magnetic field along the direction of the spins of the incident muons. Microwave power can be fed into a high-Q microwave cavity contained within the pressure vessel. Decay positrons are observed in the counter telescope 3, 4 during a time interval following the muon arrival. Observations are made as the field H is varied

Table 2. Fractional Pressure Shifts for Hfs of Hydrogen Isotopes in Argon

$\frac{1}{\Delta\nu}\frac{\partial\Delta\nu}{\partial p}$ (torr)$^{-1}$ at 0°C	
M:	$-(4.05 \pm 0.49) \times 10^{-9}$
H:	$-(4.72 \pm 0.07) \times 10^{-9}$
D:	$-(4.52 \pm 0.40) \times 10^{-9}$
T:	$-(4.72 \pm 0.07) \times 10^{-9}$

with the microwave frequency fixed. The signal will be the ratio

$$S = \frac{(3,\ 4/1,\ 2,\ \bar{3})_{\rm on}}{(3,\ 4/1,\ 2,\ \bar{3})_{\rm off}} - 1$$

($\bar{3}$ means counter 3 is anticoincident). The expression is positive at resonance.

Figure 6 shows the simple timing diagram. The pulse in the top trace is the stopped muon. The microwaves are either on continuously or off. Decay positrons are observed during a time interval ("gate") of 3 μsec, which is longer than the muon lifetime. Figure 7 is a photograph of the magnet which is a split solenoid powered by a 3/4-MW power supply with 1 part in 10^5 current regulation. It provides a field of 5000–6000 gauss homogeneous to 1 part in 10^4 over the relevant region which has dimensions of about 6 inches. Figure 8 shows the microwave system. Since a magnetic-dipole transition is being induced in a time of the order of the muon lifetime of 2 μsec, relatively high microwave power is required. The heart of the system is a klystron amplifier operating at about 1850 MHz with a cw output up to 1 kW. Power is fed into the high-Q cavity operating in the TM_{110} mode which provides a microwave magnetic field perpendicular to the static magnetic field. The frequency is stable to better than 1 part in 10^6 and the power level is stable to about 1%.

Figure 9 shows a typical resonance curve for signal as a function of static magnetic field. One-standard-deviation errors are indicated on the experimental points. The solid curve is a least-squares fit of the theoretical expression for the line shape to the experimental points. The amplitude of the signal is about 4% and agrees with the expected amplitude under the assumption that all muons form muonium. The width of the curve is about 15 gauss. It is broader than the natural linewidth of 4 gauss because of microwave power broadening, which is required to obtain a large signal. From such a curve we obtain corresponding resonance values of microwave frequency and magnetic field. We got about 12 resonance curves during successful running time of about two months. From these resonance values we can compute $\Delta\nu$ with the Breit-Rabi formula.

Figure 10 shows the results of such $\Delta\nu$ measurements as a function of argon pressure. There is clearly a substantial dependence of $\Delta\nu$ on pressure. This dependence is the so-called "hfs pressure shift" and is due to distortion of the muonium wave function in the many collisions muonium makes with argon atoms during its lifetime. The solid curve is a straight-line fit to the experimental data. The linear fit assumes that only two-body collisions and not collisions involving two argon atoms are important. Theoretical estimates of three-body collisions as well as a quadratic fit to the data support this view. The value of $\Delta\nu$ extrapolated to zero pressure is taken as $\Delta\nu$ for free muonium

$$\Delta\nu_{\rm M} = 4463.15 \pm 0.06 \text{ MHz}$$

The error of 1 standard deviation is due to counting statistics and to magnetic-field errors.

Table 2 on page 34 shows values of pressure shifts for hydrogen isotopes in argon. The muonium value is taken from the slope of the curve just shown. The other values are from optical-pumping experiments done in the pressure range around a few torr. Within the experimental error there is agreement of the muonium pressure shift with the value for H. This agreement adds assurance that the muonium pressure shift is reasonable since only a small dependence of pressure shift on isotope is expected. Better theoretical and experimental understanding of the hydrogen pressure shifts as regards both isotope dependence and possible nonlinearities might allow us to use the rather well known hydrogen pressure shift value to improve the knowledge of muonium hfs.

Last year a measurement of a transition at weak magnetic field with $\Delta F = 1$ was completed in a two-month run at Nevis. This measurement provides the most direct determination of

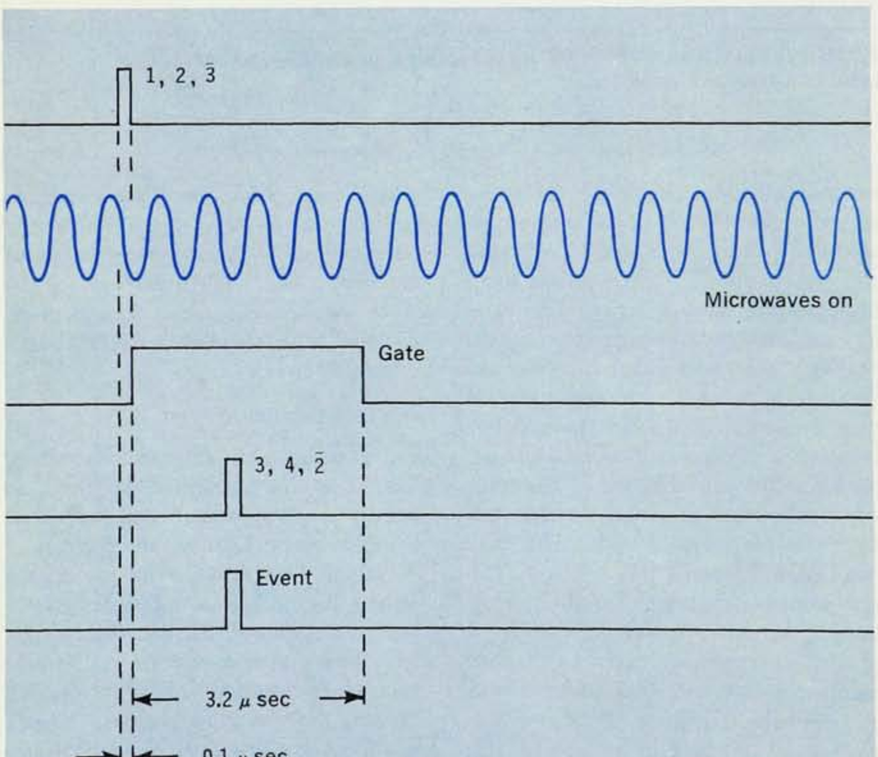

TIMING DIAGRAM for hfs transition measurement. Decay positrons are observed during a time-interval "gate" of 3.2 microsec. —FIG. 6

$\Delta\nu$. There are two principal technical problems with this experiment. First, we require a homogeneous, stable low static magnetic field near the large synchrocyclotron magnet. Second, the signal intensity is smaller than that for the strong-field transition by a factor of 5 owing to the relative populations of muonium hfs states and the small change in muon polarization accompanying the transition. Figure 11 shows the magnet arrangement. There are three molybdenum permalloy shields. Inside them are a solenoid and correction coils. This system provides an axial magnetic field of about 3 gauss with homogeneity and stability to better than 10 mG.

Figure 12 is a resonance curve for the transition $(F, M_F) = (1, -1) \leftrightarrow (0, 0)$ at 2.8 gauss fitted with the theoretical line shape. The low-field data were taken only at an argon pressure of 35 atm. From the resonance values we can compute $\Delta\nu$.

Experiment and theory

The box on page 36 summarizes the results of the muonium hfs measurements. From the high field measurement we obtain $\Delta\nu = 4463.15 \pm 0.06$ MHz. From the low field measurement we get $\Delta\nu = 4463.21 \pm 0.06$ MHz, in which the pressure shift is taken from the high field results and provides the principal source of error. The combined result is $\Delta\nu = 4463.16 \pm 0.06$ MHz. You will recall that the theoretical value based on Lamb's value of α was also 4463.16 ± 0.10 MHz, so agreement of theoretical and experimental values is excellent.

This agreement confirms the basis of the theory which was that the muon is a heavy Dirac particle or heavy electron. Since the experimental value of the hyperfine splitting is known with about the same accuracy as the theoretical value, which is limited principally by our knowledge of α, we can use the experimental value to determine an alternative value of the fine-structure constant. The theoretical formula for $\Delta\nu$ is given in more abbreviated form than before. After α, the least known constant appearing is the muon magnetic moment or actually the ratio of the muon to proton magnetic moments. This ratio is obtained from the measured ratio of the precession frequency of muons stopped

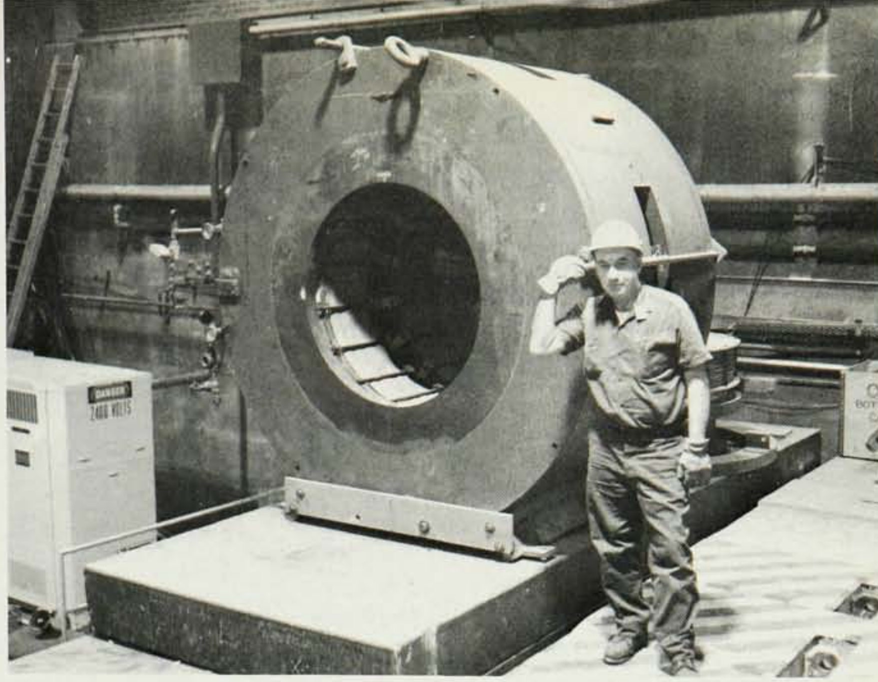

HIGH-FIELD MAGNET is a split solenoid with a 3/4-MW power supply and provides a field of 5–6 × 10³ gauss. —FIG. 7

Theoretical Line Shape

$$\mathrm{d}a_p/\mathrm{d}t = -\,i a_q b \exp(i\omega t + i\omega_0 t) - (\gamma/2) a_p$$

$$W_p - W_q = \hbar\omega_0$$

$$\mathrm{d}a_q/\mathrm{d}t = -i a_p b^* \exp(-\,i\omega t - i\omega_0 t) - (\gamma/2)\, a_q$$

Decay rate of both states p and q is γ

Initial conditions: $a_p = 1,\ a_q = 0$ at $t = 0$

$$\mathcal{H}' = \mu_0 g_J \mathbf{J}\cdot\mathbf{H}_{rf} + \mu_0 g_\mu \mathbf{I}_\mu\cdot\mathbf{H}_{rf} \qquad V_{pq} = (p|\mathcal{H}'|q) = \hbar b \exp(+i\omega t)$$

$$P_{p,q}(t) = e^{-\gamma t}\frac{|2b|^2}{|2b|^2 + (\omega_0 - \omega)^2}\sin^2\left\{\frac{1}{2}\left[|2b|^2 + (\omega_0 - \omega)^2\right]^{1/2} t\right\}$$

$$P_q = \int_0^\infty \gamma P_{pq}(t)\mathrm{d}t,$$
probability of decay from state q

$$\delta\nu = \frac{1}{\pi}(4|b|^2 + \gamma^2)^{1/2},$$ half width

$$P_q = \frac{2|b|^2}{4|b|^2 + \gamma^2 + (\omega - \omega_0)^2}$$

$\delta\nu$ (natural width) $= \dfrac{\gamma}{\pi} =$ 0.14 MHz $\approx$ 4 gauss

In the equation for $\mathrm{d}a_p/\mathrm{d}t$ the first term arises from the Hamiltonian term $\mathcal{H}'$ for the interaction of the applied time varying magnetic field with the magnetic moments of the electron and muon. The matrix element of this interaction between states p and q is $\hbar\, b e^{+i\omega t}$ for the applied field with angular frequency ω. The second term represents the effect of the decay of the muon with decay rate γ. The initial conditions are $a_p = +1$ and $a_q = 0$; that is, for the strong-field-case muonium is formed in state 1 but not in state 2. An exact solution of these equations gives the probability P_{pq} or $|a_q|^2$ that muonium is in state q at a later time t. We actually observe a portion of the decay positron angular distribution, which is proportional to the probability P_q that muonium decays from state q, and is the resonance line shape. The term $(\omega - \omega_0)^2$ gives the resonance denominator, and the line shape is Lorentzian. The half width is shown where $|b|^2$ contributes the microwave power broadening term. In the limit of zero power, we obtain the natural line width $\gamma/\pi = -0.14$ MHz, or, if the resonance line is swept by varying the magnetic field under our strong field conditions, the natural line width will be 4 gauss.

Muonium Hyperfine Structure

	High-field measurement	Low-field measurement	Average
$\Delta\nu_{\text{expt}}$ (MHz)	4463.15 ± 0.06	4463.21 ± 0.06	4463.16 ± 0.06 (1 std. dev.)

$$\Delta\nu_{\text{theor}} = \frac{16}{3}\,\alpha^2 cR_\infty \frac{\mu_\mu}{\mu_{e0}}\left(1+\frac{m_e}{m_\mu}\right)^{-3}\left[1+\epsilon\left(\alpha,\frac{m_e}{m_\mu}\right)\right]$$

$$\frac{\mu_\mu}{\mu_{e0}} = \frac{\mu_\mu\mu_p}{\mu_p\mu_e}\left(1+\frac{\alpha}{2\pi}-0.328\,\frac{\alpha^2}{\pi^2}\right)$$

$$\frac{\mu_\mu}{\mu_p} = 3.183355 \pm 0.000089 \;(\pm 28 \text{ ppm} - \text{limit of error})$$

Fine structure constant

$$\alpha^{-1} = 137.0383 \pm 0.0026 \;(\pm 19 \text{ ppm} - \text{limit of error})$$

in water to the proton resonance frequency in water. Since the chemistry of muons in water may be different from the chemistry of protons in water, principally because of the different vibrational energies, the magnetic shielding of the proton and the muon may be different. The value shown is meant to be a limit of error to take account of this ambiguity as well as two standard deviations in the experimental errors. Hence we obtain the value of α shown with a limit of error of 19 ppm.

The muonium and the old deuterium values for α are in good agreement and we can take the combined value of $\alpha^{-1} = 137.0387$ ($\pm$ 8 ppm).

α is one of the fundamental atomic constants and we need to know it well because it is significant in the whole system of fundamental constants. Moreover it is of particular importance for a comparison of experimental and theoretical values for the hfs interval in the ground state of hydrogen. The box on page 38 gives the theoretical formula for the hyperfine splitting in hydrogen $\Delta\nu_{\text{H}}$. It is very similar to that of muonium with the principal difference associated with the term δ_p. This term takes into account effects of proton structure and proton recoil, which are difficult to calculate reliably because the proton is a strongly interacting particle with a complicated structure. The term arises from an exchange of two energetic photons ($\gtrsim$ 100 MeV) between electron and proton, and the evaluation of the term is based on the high energy electron-proton elastic scattering data. The theoretical value of $\Delta\nu(\text{H})$ based on the α value just given and $\delta_p = 35$ ppm, is $\Delta\nu_{\text{theor}} = 1420.347 \pm 0.324$ MHz. The experimental value is known to 2 parts in 10^{11} from the hydrogen maser work. The values disagree by 42 ± 17 ppm in which 17 represents an error limit. There have been many recent theoretical papers which have considered the effect of proton structure on the value. The effects of a postulated axial vector meson, of a quark structure of the proton and more generally, of the polarizability of the proton have been considered. In view of the sizes of the effects calculated, we probably must say that δ_p can be uncertain theoretically by as much as 10 ppm. This uncertainty, however, is not enough to account for the difference between the theoretical and experimental values of $\Delta\nu(\text{H})$. A recent determination of e/h based on the ac-Josephson effect (see PHYSICS TODAY, **19**, no. 11, 67 1966) yields a value for α that gives excellent agreement between the theoretical and experimental values for $\Delta\nu(\text{H})$. Hence something is wrong, and a more sensitive comparison of theory and experiment awaits a better value of α.

Muonium chemistry

Muonium will behave as a light isotope of hydrogen with regard to its atomic interactions and chemical reactions since the muon mass is 207 times the electron mass and since the muon mean lifetime of 2.2 μsec is long compared to the electron atomic orbital times. In the history of the discovery of muonium, chemistry played an important negative role and many post-parity experiments that searched for the characteristic muonium precession frequency failed because of the subsequent chemical reactions of muonium with molecules. As I mentioned, we had to purify the argon gas to observe the muonium precession and the hfs transitions.

Figure 13 shows data on explicit studies of the interactions of muonium. The amplitude of the resonance signal

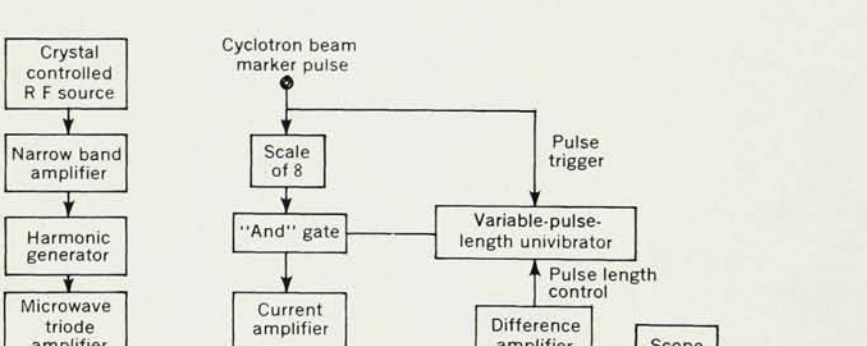

MICROWAVE SYSTEM for inducing magnetic-dipole transitions in high-field experiments. Klystron amplifier provides power at 1850 MHz.—FIG. 8

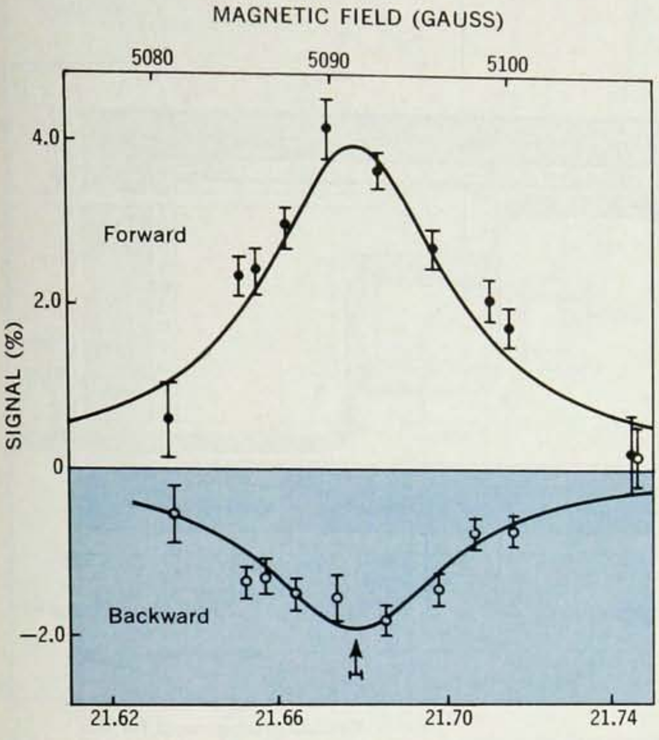

TYPICAL RESONANCE CURVES for the transition $(M_J, M_\mu) = (1/2, 1/2) \leftrightarrow (1/2, -1/2)$. Backward signal is observation of positrons emitted toward counter 2 in figure 5. —FIG. 9

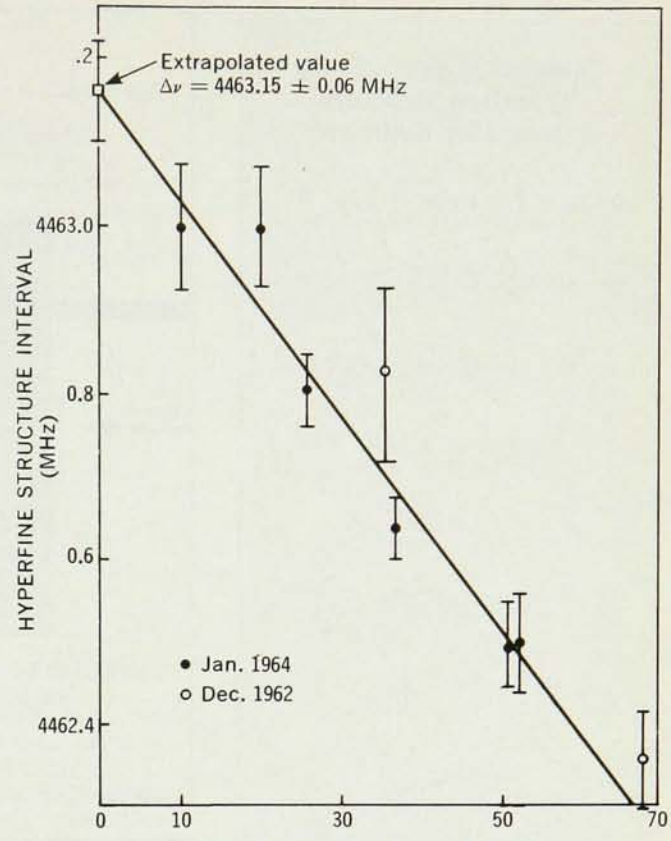

HFS INTERVAL EXPERIMENTAL value as a function of argon density. The solid line is the least-squares linear fit extrapolated to zero pressure. —FIG. 10

for a strong-field transition is shown as a function of the concentration of various molecules introduced in small fractional amounts as impurities in the argon. Note that the resonance signal is decreased by the addition of oxygen and nitric oxide, and with less effectiveness by ethylene (C_2H_4); hydrogen does not affect the signal. Decrease of the resonance signal implies collisions that remove muonium from the resonant states. In the line-shape theory the collision rate can be added to the muon decay rate and the data can be analyzed to yield a cross section for signal quenching.

For room-temperature muonium the Born-Oppenheimer approximation is valid as it is for hydrogen. As to the nature of the reactions, nitric oxide and oxygen are paramagnetic with free electron spins, and we expect that electron spin exchange will dominate. This reaction is determined by the Coulomb interaction and the Pauli exclusion principle. The exchange of the muonium electron with an argon electron can result in the transfer of muonium from one hfs state to another. Ethylene is an unsaturated hydrocarbon, and in a collision with muonium we believe that a muonium-containing molecule is formed. With hydrogen there is no reaction. Hydrogen is not paramagnetic; so electron spin exchange reactions are not possible. Furthermore a reaction such as $M + H_2 \rightarrow MH + H$ is energetically forbidden for room-temperature (thermal) muonium because of the high zero-point vibrational energy of MH.

A simpler method of studying molecular interactions of muonium involves measurement of muon polarization as a function of time and impurity concentration by use of a precision digital time analyzer following the scintillation counters. The method is of course based on a change in positron angular distribution that is a result of a change in muon polarization. Figure 14 shows such data for nitric oxide. Depolarization is plotted as a function of time during a

Table 3. Muonium-Molecule Cross Sections in 10^{-16}cm^2

Added gas	*Postulated interaction*	σ_R *from signal quenching data at 5250 gauss*	σ_{SE} *from depolarization rates at several fields*
NO_2	$+M \rightarrow NO + OM$	23 (lower limit)	—
O_2	Spin Exchange	5.4 ± 2.5	5.9 ± 0.6
NO	Spin Exchange	3.2 ± 1.5	7.1 ± 1.0
C_2H_4	$+M \rightarrow C_2H_4M$	0.29 ± 0.16	—
H_2, N_2, SF_6	—	0.01 (upper limit)	—

Theoretical Formula for Hyperfine Structure Interval for Hydrogen

$$\Delta\nu_{\text{theor}} = \left(\frac{16}{3}\alpha^2 c R_\infty \frac{\mu_p}{\mu_{e0}}\right) \times \left(1 + \frac{m_e}{m_p}\right)^{-3} \times \left(1 + \frac{3}{2}\alpha^2 + a_e + \epsilon_1 + \epsilon_2 + \epsilon_3\right)\left(1 - \delta_p\right)$$

$$a_e = \frac{\alpha}{2\pi} - 0.328\frac{\alpha^2}{\pi^2};$$

$$\epsilon_1 = \alpha^2\left(\log 2 - \frac{5}{2}\right)$$

$$\epsilon_2 = -\frac{8\alpha^3}{3\pi}\ln\alpha\left(\log\alpha - \log 4 + \frac{281}{480}\right)$$

$$\epsilon_3 = \frac{\alpha^3}{\pi}\left(18.4 \pm 5\right)$$

$\delta_p = 35 \times 10^{-6}$ (proton recoil and proton structure)

$\alpha^{-1} = 137.0387$ (± 8 ppm: error limit); $R_\infty = 109\,737.31$ cm^{-1} (± 0.1 ppm)

$\frac{\mu_e}{\mu_p} = 658.2106$ (± 1 ppm);

$\frac{m_p}{m_e} = 1836.12$ (± 11 ppm)

$c = 2.997925 \times 10^{10}$ cm/sec (± 0.3 ppm)

$\Delta\nu_{\text{theor}} = 1420.347 \pm 0.024$ MHz (± 17 ppm: error limit)

$\Delta\nu_{\text{expt}} = 1\,420\,405\,751.800 \pm 0.028$ Hz

$\frac{\Delta\nu_{\text{expt}} - \Delta\nu_{\text{theor}}}{\Delta\nu_{\text{expt}}} = 42 \pm 17$ ppm (error limit)

δ_p(theor) uncertain by about 10 ppm

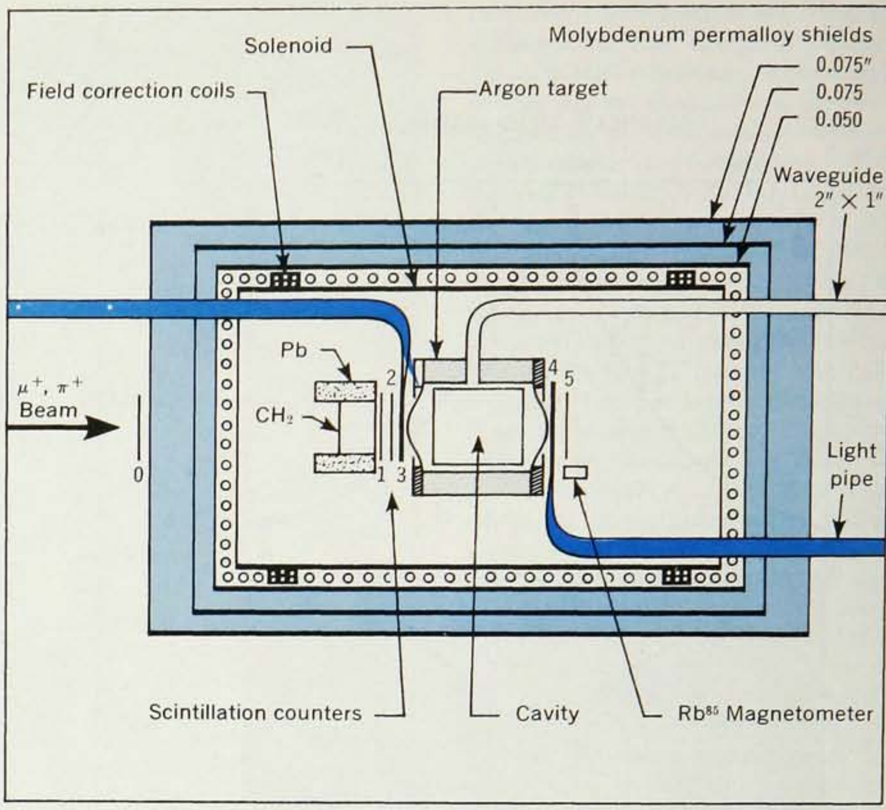

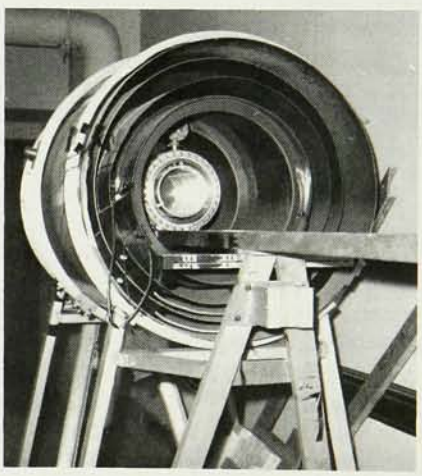

LOW-FIELD arrangement for hfs interval measurement. Photo at left shows target. —FIG. 11

period of several muon mean lives for two different nitric oxide concentrations; for the lower curve the pressure of nitric oxide was 0.13 torr and for the upper curve, 0.37 torr. Typical statistical errors are shown. The solid curves are simple exponential functions. If the reaction mechanism is electron spin exchange, the theoretical curve is an exponential and the coefficient of the exponent is proportional to the electron spin exchange cross section. Figure 15 shows similar data for ethylene, again fitted by exponentials. The effective cross section is smaller than for nitric oxide.

A more detailed study of the nature of the depolarizing collisions can be made by observation of the depolarization rate as a function of the static magnetic field. At strong field an electron-spin-exchange collision will leave the muon spin direction unchanged and hence the effective depolarizing cross section will be zero. At weak field, on the other hand, the coupling of the electron and muon spins by the hfs interaction results in a change of muon spin direction when an electron spin exchange occurs. The variation of depolarizing cross section as a function of magnetic field depends only on the spin eigenfunctions and is simply predicted. Figure 16 shows data for nitric oxide, which has a single free electron spin—$^2\Pi$ state—as a function of H. The depolarization factors is $1 - e^{-\lambda t}$, where λ is the fitted depolarization rate, under the assumption that the muon depolarization varies as $P = P_0 e^{-\lambda t}$. The experimental points are in good agree-

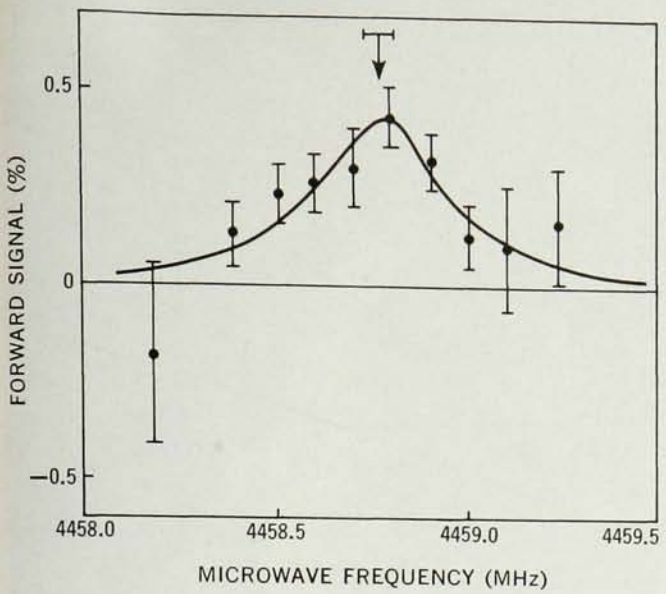

RESONANCE CURVE for the transition $(F,M_F) = (1,-1) \leftrightarrow (0,0)$ at a field of 2.8 gauss. —FIG. 12

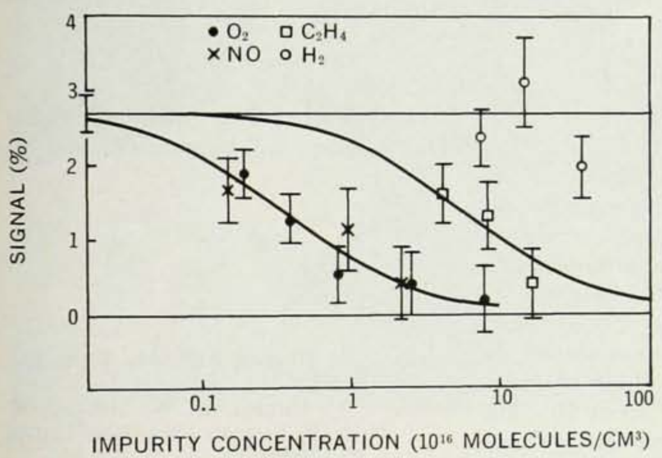

IMPURITY AFFECT. Resonance signal for the transition $(M_J,M_\mu) = (1/2,1/2) \leftrightarrow (1/2,-1/2)$ at 5200 gauss as a function of impurity concentration. Solid lines are fitted theoretical curves that involve the signal quenching cross section as a parameter. —FIG. 13

Muonium-Antimuonium Conversion

$$\mu^+e^- \to \mu^-e^+$$

violates additive law of muon conservation.

Allowed by multiplicative law of muon conservation:

$$\mathcal{H} = G_{M\bar{M}}\bar{\psi}_\mu\gamma_\lambda(1 + \gamma_5)\psi_e\bar{\psi}_\mu\gamma^\lambda \times (1 + \gamma_5)\psi_e$$

$$(\bar{M}|\mathcal{H}|M) = \frac{\delta}{2} = \frac{8G_{M\bar{M}}}{\pi a_0^3}$$

(for $G_{M\bar{M}} = G_V$, $\delta = 2.1 \times 10^{-12}$ eV)

$$\psi(t) = a\phi_M + b\phi_{\bar{M}} \quad (\text{at } t = 0,\ a = 1,\ b = 0)$$

$$P(\bar{M}) = \frac{\delta}{2\Lambda^2}\left(\frac{G_{M\bar{M}}}{G_V}\right)^2 = 2.6 \times 10^{-5}\left(\frac{G_{M\bar{M}}}{G_V}\right)^2$$

(in vacuum)

where $\Lambda = \hbar\gamma$

$$P_{\text{gas}}(\bar{M}) \approx \frac{1}{N} P_{\text{vac}}(\bar{M})$$

$$\bar{M} + A \to \mu^- A$$

$$G_{M\bar{M}} \lesssim 2 \times 10^5 G_V$$

ment with the theoretical solid curve and hence the spin-exchange nature of the collision is confirmed. Similar confirmation has been established for oxygen.

Table 3 summarizes the data on muonium-molecule cross sections obtained thus far. For nitrogen dioxide we believe the reaction is

$$NO_2 + M \to NO + OM$$

We should note that for oxygen and nitric oxide the reaction mechanism is an electron spin exchange. Corresponding spin exchange cross sections for hydrogen with nitric oxide and oxygen, $[(21 \pm 2.5) \times 10^{-16}$ cm^2 and $(21 \pm 2.1) \times 10^{-16}$ cm^2, respectively$]$, measured with the use of the hydrogen maser, are about 3 or 4 times larger than for muonium. We believe that this difference is because muonium and hydrogen have different momenta for a given kinetic energy and hence different numbers of partial waves contribute to the reaction. For the ethylene reaction we believe that a muonium-containing molecule is formed. No reaction was observed for hydrogen, nitrogen and sulfur hexafluoride SF_6. The absence of a reaction for hydrogen was discussed and similar remarks apply to nitrogen.

Our work on muonium chemistry is in an early stage and a rich variety of reactions could be studied and compared with those of hydrogen. Indeed in some ways muonium chemistry is easier to study than hydrogen atom chemistry.

Conversion to antimuonium

Muonium provides an interesting system for study of the weak interactions and the nature of the muon quantum number. The conversion of muonium to antimuonium (μ^-e^+) would violate the usual additive law of muon number conservation but would be allowed by a multiplicative law of muon number conservation, which would be consistent with present knowledge about the weak interactions (box on page 39). A Hamiltonian term which couples muonium ($\bar{M}$) and antimuonium (M) is shown, and value of the matrix element is shown for the case in which the coupling constant is taken as the universal Fermi constant G_V. M and $\bar{M}$ are degenerate as regards their electromagnetic interaction. If initially M is formed, then due to the coupling term $\mathcal{H}$ a component of $\bar{M}$ is formed in the wavefunction. Hence there is a probability that muon decay will occur in the $\bar{M}$ mode with

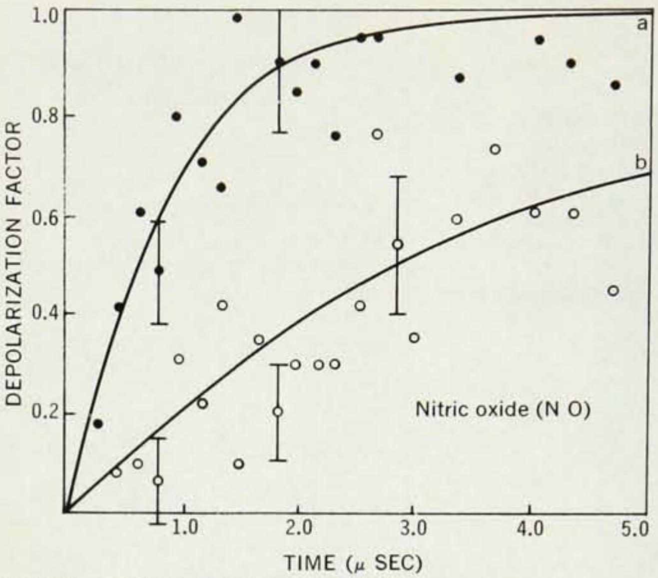

DEPOLARIZATION FACTOR as a function of time for nitric oxide. —FIG. 14

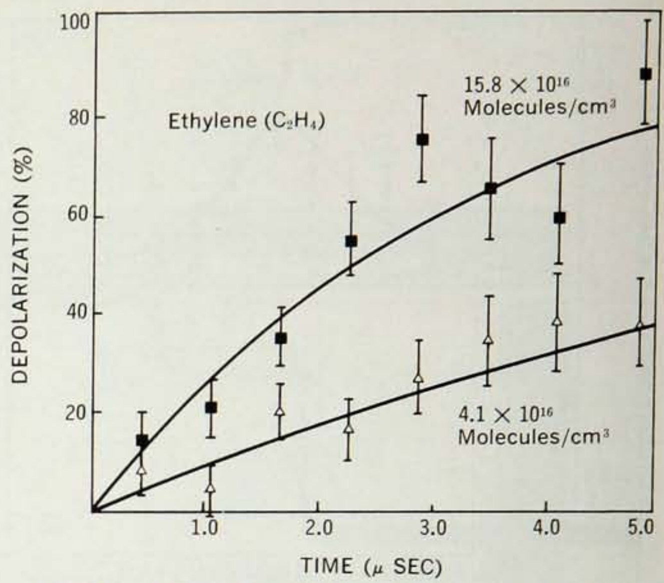

DEPOLARIZATION FACTOR as a function of time for ethylene. —FIG. 15

the emission of an energetic electron. The probability $P(\overline{M})$ is 2.6×10^{-5} for muonium in vacuum. In the presence of a gas the degeneracy of M and $\overline{M}$ is removed due to the different electromagnetic interactions of $\overline{M}$ and M with atoms for example, argon. Hence the development of the $\overline{M}$ component is inhibited, and $P(\overline{M})$ is reduced by the factor $1/N$, the number of collisions of the M-$\overline{M}$ system with argon atoms during its lifetime. Furthermore, the argon gas will change the mode of $\overline{M}$ decay. In a gas $\overline{M}$ would form the mu-mesic argon atom. We are planning an experiment to search for the characteristic mu-mesic argon x-rays as a sensitive test for the $M \rightarrow \overline{M}$ conversion.

At present the best estimate of $G_{M\overline{M}}$ is obtained from knowing that muonium has approximately the lifetime of the free positive muon, as evidenced by all the experiments on muonium, including the muonium precession and hfs measurements. We know only that $G_{M\overline{M}} < 2 \times 10^5 \, G_v$.

As to future work on muonium, let me just remark that all our work has been done with only about 10^{10} muonium atoms; work on the hydrogen atom on the other hand, has available hydrogen atom beam intensities of 10^{14} atoms/sec. Research on muonium is now severely limited by the number of muonium atoms available and by muon beam intensities. When higher-intensity accelerators—so-called meson factories—get built, great improvements and extensions of studies of muonium will be possible.

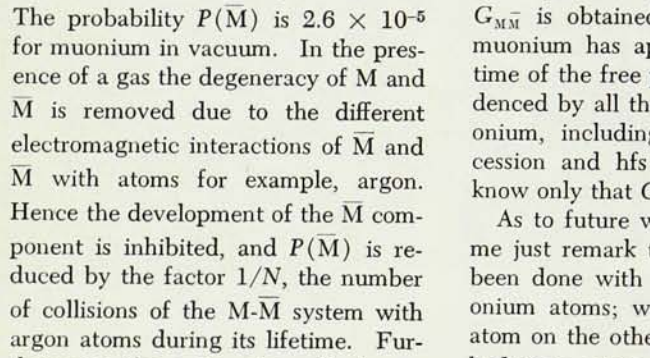

SPIN-EXCHANGE theory fitted to data for nitric oxide molecule. Depolarization rate per impurity molecule (λ/n) is shown as a function of *H*. —FIG. 16

Bibliography

1. V. W. Hughes, Bull. Am. Phys. Soc. **2**, 205 (1957).
2. V. W. Hughes, D. W. McColm, K. Ziock, R. Prepost, Phys. Rev. Letters **5**, 63 (1960).
3. R. Prepost, V. W. Hughes, K. Ziock, Phys. Rev. Letters **6**, 19 (1961).
4. K. Ziock, V. W. Hughes, R. Prepost, J. M. Bailey, W. E. Cleland, Phys. Rev. Letters **8**, 103 (1962).
5. W. E. Cleland, J. M. Bailey, M. Eckhause, V. W. Hughes, R. M. Mobley, R. Prepost, J. E. Rothberg, Phys. Rev. Letters **13**, 202 (1964).
6. P. Thompson, J. Amato, V. W. Hughes, R. Mobley, J. Rothberg, Bull. Am. Phys. Soc. **11**, 343 (1966).
7. R. M. Mobley, J. M. Bailey; W. E. Cleland, V. W. Hughes, J. E. Rothberg, J. Chem. Phys. **44**, 4354 (1966).
8. D. Morgan, Bull. Am. Phys. Soc. **9**, 393 (1964).
9. V. W. Hughes, Ann. Rev. Nucl. Sci. 16, 445 (1966).
10. V. W. Hughes, Scientific American **214**, no. 4, 93 (1966).
11. P. Thompson, J. J. Amato, V. W. Hughes, R. M. Mobley, J. E. Rothberg, Bull. Am. Phys. Soc. **12**, 75 (1967).
12. R. M. Mobley, J. J. Amato, V. W. Hughes, J. E. Rothberg, P. Thompson, Bull. Am. Phys. Soc. **12**, 104 (1967). □